Construction and Kinematic Analysis of an Anthropomorphic Mobile Robot

Scott Nortman, Jack Peach, Michael Nechyba, Louis S. Brown, A. Arroyo
Machine Intelligence Laboratory
University of Florida
Gainesville, FL

FCRAR
May 10-11, 2001
FAMU

Construction and Kinematic Analysis of an Anthropomorphic Mobile Robot

Scott Nortman, Jack Peach, Michael Nechyba, Louis S. Brown, A. Arroyo
Machine Intelligence Laboratory
University of Florida
Gainesville, FL

Abstract

This paper discusses the development, design, and initial construction of an autonomous anthropomorphic mobile robot currently being developed at the University of Florida's Machine Intelligence Laboratory (MIL). Additionally, the forward and inverse kinematics of the five-degree of freedom manipulator arms are solved.

Design and Construction

The concept for this robot evolved from a previous project developed at the University of Florida during summer 1999. The previous robot, Omnibot 2000, was designed to aid the elderly and handicapped, as well as to entertain an audience and give tours of the MIL. Due to the Omnibot's success, a grant was provided by the Department of Electrical and Computer Engineering to design and build an improved version of the platform. This new platform, called Pneuman, will improve Omnibot's features, and will be capable of performing more complex tasks.

The initial mechanical platform was conceived in September 1999 (Figure 1). This design had 15 degrees of freedom (DOF), and intended to use pneumatic cylinders and compressed air for a majority of its actuators. There were 14 pneumatic cylinders and eight DC motors. Seven of the 15 degrees of freedom used two pneumatic cylinders working simultaneously to allow the DOF 180 degrees of motion. This was accomplished by arranging the cylinder pairs 90 degrees out of phase. This allowed one of the cylinders to exert its maximum amount of force while the other cylinder could not exert any force because its moment arm would go to zero at 0 and 180 degrees (Figure 2). Electronic cylinder control modules were developed, utilizing solenoid valves. These control devices were interfaced to a host processor implementing a PID control algorithm.

Figure 1

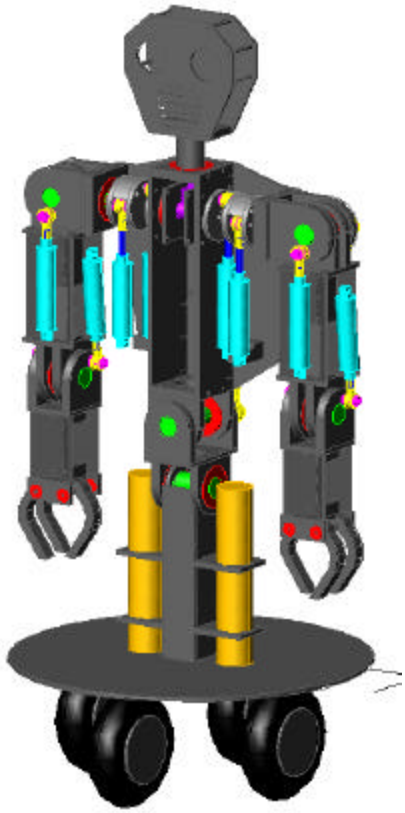

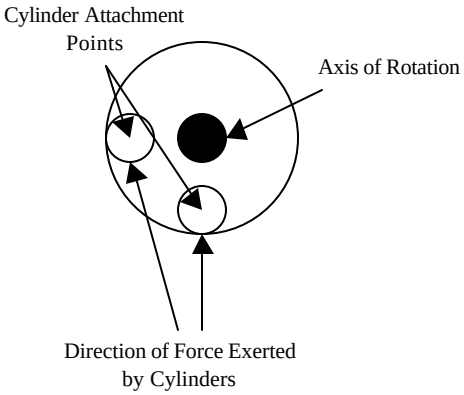

Figure 2

Two SpareAir© tanks were to provide pressurized air to the pneumatic actuators via a regulator. The tanks were pressurized to 3000 PSI and the regulator would drop the system pressure to 100 PSI. The regulated air was sent through a series of needle valves to adjust the flow rate. This allowed the cylinders to move at a reasonable rate of speed.

The initial concept design was evaluated and modified by two mechanical engineering students during the spring semester of 2000. Their new design is shown in Figure 3.

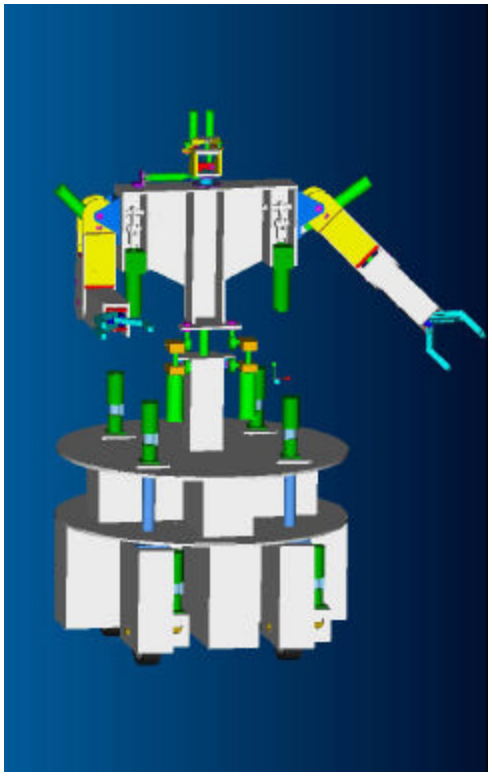

Figure 3

This new platform had two design flaws. First, the overall mechanical structure was too heavy. Because the robot is autonomous, consideration should have been given to the weight of the structure. Unnecessary weight will limit to robot's mobility and shorten its battery life. Furthermore, due to the significant overhead required to operate and maintain the pneumatic actuation system, an alternate method of actuation was sought. Therefore, DC motors are currently being used throughout the entire robot. These two factors led to a third revision of the platform shown in Figure 4.

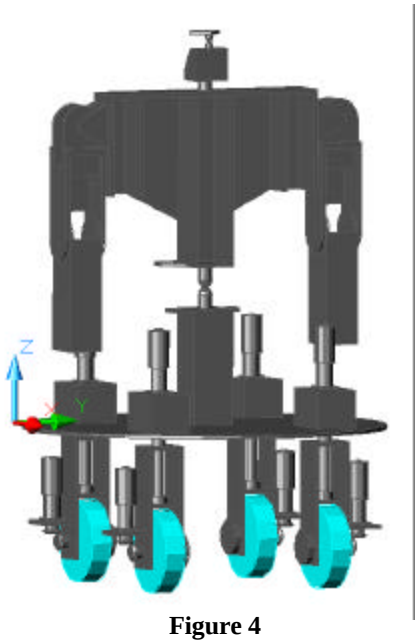

Figure 4

One last modification was made to the above platform. The change includes the replacement of the arms with more dexterous arms that have 5 DOF and a dexterous hand. This final revision of the platform is currently being constructed at the MIL. A prototype of the new arm is shown in Figure 5.

Figure 5

5 DOF Arm

Overview

The two arms discussed below are five degree-of-freedom (5 DOF) serial link manipulators. Constructed from aluminum and plastic, the arms were designed to perform similar to human arms. Upper and lower arm lengths are proportional to that of an adult human. Explosion of kinematics equations were kept to a minimum by aligning the axis of rotation from joint to joint. As shown above in Figure 4, the arms are mirror images of each other and are identical in all other respects.

Joint Configuration

When designing a higher nth order DOF serial link manipulator, one must consider the kinematics equations behind each joint placement. The arm was designed so that joint axis *i* intersects joint axis *i+1*, where *i* is the number of joints in the arm. Each new link is offset from the previous link by 90° as shown in Figure 6. Additionally, see Table 1 for joint characteristics.

Joints ShoulderA, ShoulderB, and ElbowA are coincident at the shoulder. This alignment allows for the arm to rotate as if a ball and socket joint were implemented. ElbowB and WristA joints are also coincident. Joints ShoulderA, ShoulderB, and ElbowB are actuated by linear actuators. The remaining joints, ElbowA and WristA, are actuated by rotary actuators.

Figure 6
Arm kinematics. The arrows indicate direction of rotation. The thick lines represent the links.

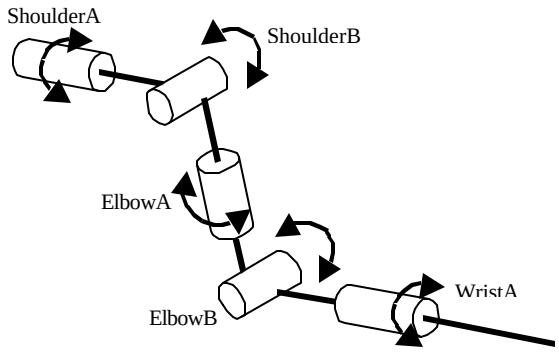

Joint	Max Torque (Nm)	Max Speed (rpm)	Range of Motion (degrees)
ShoulderA	14.00	10	120
ShoulderB	14.00	10	90
ElbowA	10.00	20	90
ElbowB	10.00	10	120
WristA	1.00	20	180

Table 1: Joint Characteristics

Kinematic Analysis of Arm

DH Parameters

Figure 7, shown below, indicates which frames correspond to each linkage. Note that frame {0} is coincident with frame {1} when $\theta_1 = 0$.

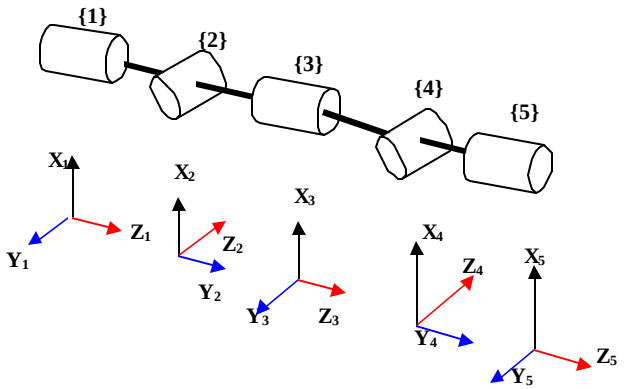

Figure 7

The DH parameters are shown in Table 2 below.

I	α_{I-1}	a_{i-1}	d_i	q_I
1	0	0	0	θ_1
2	$\pi/2$	0	0	θ_2
3	$-\pi/2$	0	d_3	θ_3
4	$\pi/2$	0	0	θ_4
5	$-\pi/2$	0	0	θ_5

Table 2

The base frame {0} is positioned at the shoulder. This is the arm's point of attachment to the body of Pneuman. The origin of frame {5} is located at the wrist. A dexterous hand will be attached here in the future.

Forward Kinematics

The overall forward kinematics for the manipulator is given by the transform

$$ {}^{0}_{5}T = \begin{bmatrix} r_{11} & r_{12} & r_{13} & p_x \\ r_{21} & r_{22} & r_{23} & p_y \\ r_{31} & r_{32} & r_{33} & p_z \\ 0 & 0 & 0 & 1 \end{bmatrix} $$

where

$r_{11} = c_5[c_4(c_1c_2c_3-s_1s_3)-c_1s_2s_4]-(c_3s_1+c_1c_2s_3)s_5$
$r_{12} = -c_5(c_3s_1+c_1c_2s_3)-[c_4(c_1c_2c_3-s_1s_3)-c_1s_2s_4]\ s_5$
$r_{13} = -c_1c_4s_2-(c_1c_2c_3-s_1s_3)s_4$
$r_{21} = c_5[c_4(c_2c_3s_1+c_1s_3)-s_1s_2s_4]-(c_2s_1s_3-c_1c_3)s_5$
$r_{22} = -c_5(c_2s_1s_3-c_1c_3)-[c_4(c_2c_3s_1+c_1s_3)-s_1s_2s_4s_5]$
$r_{23} = -c_4s_1s_2-(c_2c_3s_1+c_1s_3)s_4$
$r_{31} = c_5(c_3c_4s_2+c_2s_4)-s_2s_3s_5$
$r_{32} = -c_5s_2s_3-(c_3c_4s_2+c_2s_4)s_5$
$r_{33} = c_2c_4-c_3s_2s_4$
$p_x = -d_3c_1s_2$
$p_y = -d_3s_1s_2$
$p_z = d_3c_2$

Note that d_3 is the distance between ShoulderB (frame {2}) and ElbowA (frame {3}). Also note that the origin of the frame for ElbowA is the same as the origin of the frame for ElbowB (frame {4}).

Inverse Kinematics

After the forward kinematics solution was determined, the closed form inverse kinematic solution was found for the 5 DOF arm. The solutions for the joint angles are

$$\theta_1 = \text{Atan2}[-p_y, -p_x]$$

$$\theta_2 = \text{Atan2}\left[\pm\sqrt{p_x^{\,2} + p_y^{\,2}}, p_z\right]$$

$$\theta_3 = \text{Atan2}[(-r_{12}c_1c_2+r_{23+}s_1c_2+r_{33}s_2), r_{12}s_1-r_{23}c_1]$$

$$\theta 4 = \text{Atan2}\left[\left(\pm\sqrt{(r_{31}c_2-(r_{11}c_1+r_{21}s_1)s_2)^2+(r_{32}c_2-(r_{12}c_1+r_{22}s_1)s_2)^2}\right), (r_{33}c_2-r_{12}c_1s_2-r_{23}s_1s_2)\right]$$

$$\theta_5 = \text{Atan2}[(c_3(r_{21}c_1-r_{11}s_1)-(r_{11}c_1c_2+r_{21}s_1c_2+r_{31}s_2)s_3), (c_3(r_{22}c_1-r_{12}s_1)-(r_{12}c_1c_2+r_{22}s_1c_2+r_{32}s_2)s_3)]$$

The 5 DOF arm was also simulated in Mathematica. An image is shown in Figure 7. Note that the base frame {0} is at the lower potion of the image and that the wrist frame {5} is at the top of the image.

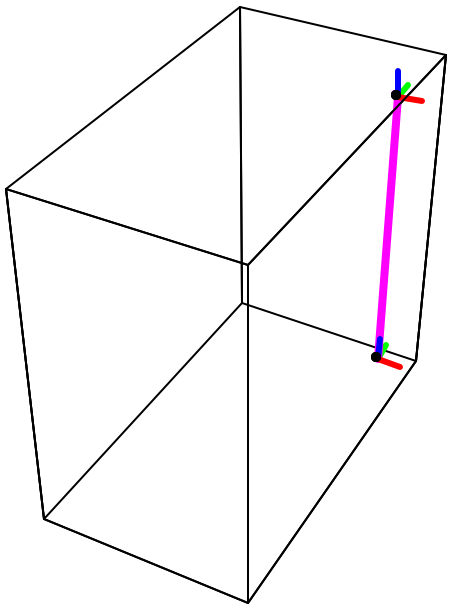

Figure 7: 5 DOF Mathematica Simulation

Two additional simulations were performed. The first, shown in Figure 8, illustrates the reachable workspace of the manipulator arm with the following joint limitations:

$0 < \theta_1 < 180°$
$0 < \theta_2 < 180°$
$0 < \theta_3 < 180°$
$0 < \theta_4 < 180°$
$0 < \theta_5 < 180°$

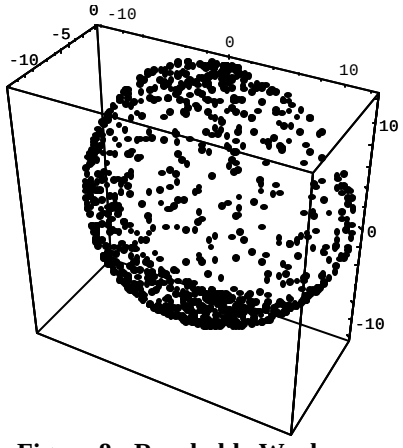

Figure 8: Reachable Workspace

Note that each black dot indicates a random vector **Q** for the joint angles, where

$$\mathbf{Q} = [\theta_1, \theta_2, \theta_3, \theta_4, \theta_5]^T$$

The final simulation in Figure 9 represents the possible orientations of the manipulator.

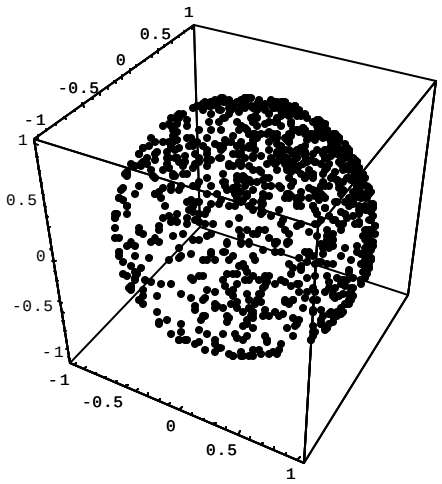

Figure 9: Possible Orientations

Again, each black dot indicates a random vector **Q** for the joint angles.

Actuators

After weighing the pros and cons of a number of actuator schemes, it was found that DC motors would provide the needed torque with the least complexity. However, DC motors present problems when implemented in robotic systems. These complex systems rely on precision and repeatability. DC motors produce backlash, which throws off precision and thereby repeatability. To help remedy this problem a revolute series elastic actuator (SEA) has been devised (Figure 10). The revolute SEA will reduce backlash and will provide force feedback at the joint. The SEA also promotes robustness and compliance throughout the arm. Figure 7 depicts a basic representation of a SEA. A spring is placed inline with the transmission shaft to reduce unwanted backlash and problems that may arise due to a sudden impact of a link with an object.

Two brands of surplus motors were purchased; one having a stall torque of 320 oz.-in. and the other 200

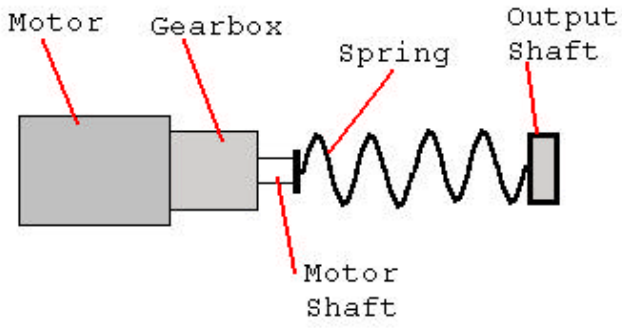

Figure 10: Series elastic actuator (SEA)

oz.-in. Although these motors would suffice, gear reduction at specified joints was imminent. Two joints that did not require any gear reduction other than that of the gearbox were ElbowA and WristA. Directly driven, these two joints proved more than the required range of motion and max speed. Table 3 describes the characteristics of the DC motors.

Joint	Voltage (volts)	Stall Torque oz in	Max Speed (rpm)
ShoulderA	24	320	120
ShoulderB	24	320	120
ElbowA	12	200	22
ElbowB	24	320	120
WristA	12	200	22

Table 3: DC motor characteristics.

Rotary Actuator

One of the problems encountered when designing the rotation aspects of the upper arm was to align the ShoulderB joint perpendicular with the ElbowB axis. A pulley drive system was implemented to overcome this problem. The advantage of a pulley drive system is its compactness compared to the linear actuator. In a pulley drive system there is no need for a lever arm or a lead screw. Another advantage over the lead screw is that it increases the available rpm at the joint it actuates. The SEA's axis of rotation is coincident with that of the joint's axis. Below in Figure 11 the motor pulley is rigidly attached to the motor shaft. The cable is wrapped around the motor pulley and partly around the joint pulley. Both ends of the cable are terminated on the joint pulley. One is static while the opposite end is attached to a cable-tensioning device. The cable-

tensioning device is necessary to keep the cable taut at all times. An "intelligent" tensioning device such as an inline memory-shape alloy extension spring may be implemented in a later version of the rotary actuator.

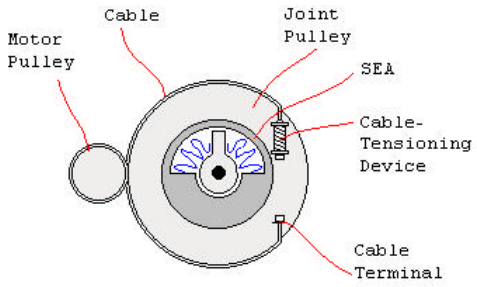

Figure 11: Rotary actuator drive system

Sensors

Joint Angles

Information regarding joint angle position will be obtained by potentiometers. The sensors will be aligned with the axes of rotation for all of the joints, providing an analog voltage proportional to the joint angle.

Force Feedback Mechanism

Robot manipulator arms are precise when it comes to movement, yet are poor at sensing applied force. When a manipulator arm is exposed to an object either intentionally or unintentionally, it has no way of sensing the applied force unless equipped with a force sensor. Force sensors are used to regulate arm motion, but may also be used to deal with contact forces. In order to overcome this shortfall in our robot arms, force-sensing resistors (FSR) have been imbedded within the rotary SEA to provide sufficient force feedback.

The static mechanics in Figure 12 are as follows:

- The motor is rigidly attached to link A.
- 'A' is rigidly attached to the motor shaft.
- 'B' is rigidly attached to link B.
- Two FSR are rigidly attached to opposite sides of the inner wall of 'B'.
- Both ends of the spring are rigidly attached the individual FSR surfaces.

Note that the motor shaft will not be attached directly to 'A'. A pulley system will interface between 'A' and the motor shaft thereby increasing output torque.

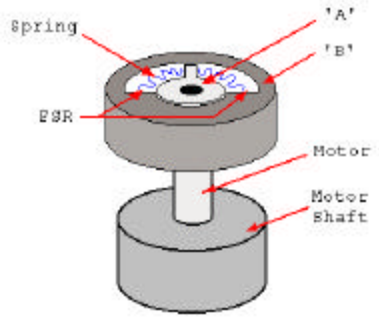

Figure 12: Series elastic actuator (SEA) with motor

Now, a dynamic description of Figure 13:

- Zero-force operation:
  - When the motor rotates, 'A' and 'B' are coincident and will rotate together.

- Force-sensing operation:
  - When the motor rotates, 'A' will rotate yet resisting force on link B will not allow 'B' to rotate. Therefore, the spring will compress.
  - When the spring compresses, the FSR senses a change in force applied. This change in applied force is linearly related to the change in rotation between 'A' and 'B'.

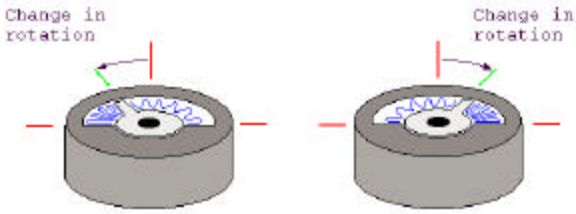

Figure 13: SEA Dynamics

Software and Electronics

The electronics system of Pneuman may be broken down into blocks. The main processor is a ZF Linux 486 PC/104 embedded computer. It is running the Red Hat Linux 5.2 operating system. This computer interfaces to six PC/104 cards. Three of the PC/104 cards generate the pulse width modulation (PWM) signals, motor direction signals, and have analog to digital inputs for all of the motors on Pneuman. The fourth card contains four National Semiconductor LM629 PID motion controller IC's. This card controls the drive motors that use an optical encoder for feedback. The fifth card is an RC Systems VX860 voice synthesizer card. This card allows Pneuman to talk. The final PC/104 card is a PCMCIA to PC/104 bus adaptor card that allows the use of a wireless networking card.

The PC/104 PWM cards were custom designed for Pneuman (Figure 14). The boards have three main systems, including PWM components, digital input/output (IO) components, and an analog to digital converter. The goal for the boards is to provide a complete PID controller for each motor implemented in software. This will be possible by using the analog inputs for angle position sensors, and controlling the motors via a motor driver board with PWM and direction signals.

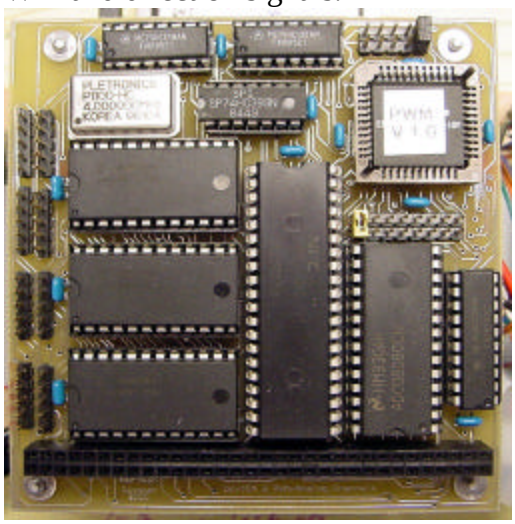

Figure 14: PWM Board

The first system is responsible for generating PWM using three standard 8254 programmable timers. Each timer chip contains three individual timers, for a total of nine timers on each PC/104 board. Each timer has a count register associated with it. Depending on the mode of operation, when the count register counts down to zero, an event may occur. One of the timers is set to operate as a real-time interrupt (RTI) providing a signal that corresponds to the period of the PWM signals. Note that all eight of the PWM signals generated must have the same period. This RTI signal is connected to the trigger inputs of all the other timers. Furthermore, all of the other timers (eight) are operating in "one-shot" mode. This means that once the trigger is asserted, the outputs of these timers are asserted until their count registers have reached zero, thereby de-asserting the output. Additionally, the values in the count registers are loaded with different values via the PC/104 bus, thereby changing the time that the outputs are high. Thus, this may be used in combination with the RTI as mentioned above for hardware PWM.

The next system provides eight digital IO's for the direction of each motor, eight outputs to control the A to D, and eight inputs to read the A to D values. This system uses a standard 8255 PPI IC. The final component of the board uses an Analog Devices ADC0808 IC. This particular IC provides eight input channels as well as eight bits of resolution for each channel.

The PC/104 LM629 PID motor controller board was also custom designed for Pneuman (Figure 15). The boards have four controller IC's. The 486 computer interfaces to these IC's via the PC/104 bus. They are dedicated motion control processors that use a quadrature incremental position feedback signal. Optical encoders mounted directly to each drive wheel provide these signals. There are four eight-bit PWM outputs for directly driving an H-bridge motor driver. Each IC may operate in position or velocity mode. Position mode will be useful for doing navigation through dead reckoning.

Velocity mode will insure that the wheels are all operating at the same speed.

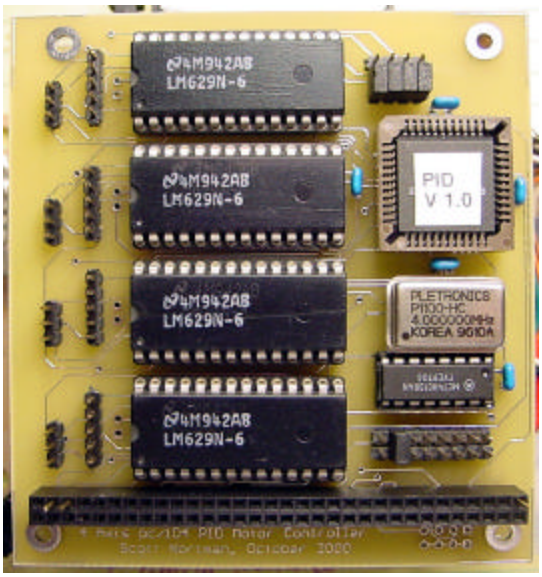

Figure 15: PID PC/104 Board

Software Subsystem

The code on the embedded 486 computer is being developed in the C programming language for the Linux 5.2 operating system. The code consists of six modules, all of which are individual processes (Figure 16). The main executable is a process manager that initializes memory space for the other processes and executes the requested modules. The communication module is necessary for control of the serial ports.

The results from the processes are then sent to the other modules via a shared memory space. The movement control module keeps precise records of the current states of all the actuators. This data is used to determine what control is necessary to move to a desired position. The data analysis module will contain the primary functions for all of the data processing. This module enables autonomous control of the entire system. All the other modules contain the data input and output functions, providing the data analysis module with all the necessary parameters. A debug module is included in the design, enabling human intervention into the control of the platform. The debug module provides a screen image of all the data gathered by the system and allows an override of any control parameters.

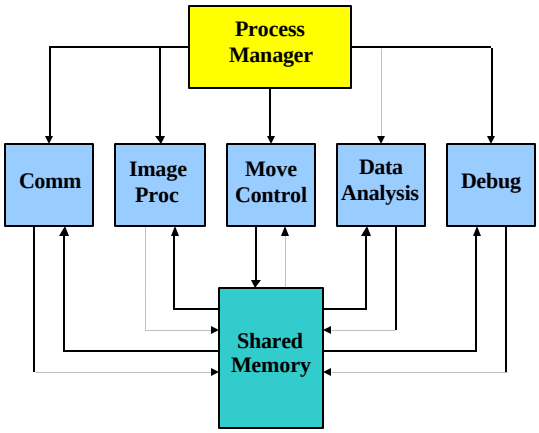

Figure 16: Software Architecture

Conclusion

Building Pneuman has provided the MIL with an excellent opportunity to design and construct a physical platform. After Pneuman is finished, this student built platform will be a part of the MIL and will foster other students' research. It will provide tours of the labs for prospective engineering students. Because this platform is available to other students, they can implement their new ideas with ease and see them in their final form.

Although simulations are useful for determining the feasibility of a concept, the construction of a prototype provides more information and experience with robotics. This, along with the gratification of seeing student ideas become implemented in a physical robot make Pneuman an excellent learning tool. This is evident from the work presented, and will be obvious when the platform is finished.

References

[1] Craig, J. J., *Introduction to Robotics: Mechanics and Control, 2nd ed.,* Addison-Wesley, Reading, MA 1989.

[2] Nortman, Scott, A. Arroyo, E. Schwartz, *Omnibot 2000*: Development of an Autonomous Mobile Agent for the Disabled and Elderly, *Florida Conference on Recent Advances in Robotics*, Dania, Florida, 2000.

[3] Nortman, Scott, S. M. Kanowitz, A. Arroyo, E. Schwartz, Development Of An Anthropomorphic Mobile Agent, *Florida Conference on Recent Advances in Robotics*, Dania, Florida, 2000.

[4] Williamson, M. M., *Series Elastic Actuators*, Master's Thesis, Massachusetts Institute of Technology Artificial Intelligence Lab, Cambridge, MA, 1995.